Carbohydrate Polymers 103 (2014) 234–243

Contents lists available at ScienceDirect

Carbohydrate Polymers

journal homepage: www.elsevier.com/locate/carbpol

Influence of glucan structure on the swelling and leaching properties of starch microparticles

Nicolas Bordenave [1], Srinivas Janaswamy, Yuan Yao *

Department of Food Science, Purdue University, 745 Agriculture Mall Dr., West Lafayette, IN 47907, United States

ARTICLE INFO

Article history:
Received 30 April 2013
Received in revised form
21 November 2013
Accepted 25 November 2013
Available online 4 December 2013

Keywords:
Starch
Microparticle
Swelling
Leaching
Crystallinity
Response surface method
Molecular weight

ABSTRACT

Microparticles were made by a water-in-oil emulsion technique from acid-hydrolyzed and debranched normal, waxy and high-amylose corn starches. The starches prepared had a weight-average molecular weight (M_w) ranging 3.6×10^7–2.5×10^4, a polydispersity ranging 1.16–9.16, an apparent amylose content ranging 2.84–100%. These microparticles exhibited crystallinity ranging 4.41–22.84%, swelling power ranging 2.45–7.84 and percentage of leaching ranging 1.72–74.91%. Swelling power in water ($R^2 = 0.86$) and percentage of leaching in water ($R^2 = 0.89$) were modeled by a response surface method, using the following parameters: M_w, polydispersity, apparent amylose content and crystallinity of starch in microparticles. Overall, this study showed the key parameters for controlling the behavior of starch microparticles were related to the cohesiveness of the three-dimensional network, particularly through the retrogradation of starch polymers, the formation of crystallites and junctions zones. Such microparticles could be used for designing economical and biocompatible delivery systems of compounds for food, drug, or other applications.

1. Introduction

Over the last decades, polymer-based delivery systems have gained considerable interest. These systems, commonly based on the formation of hydrogels from synthetic or natural polymer, have been extensively studied and developed (Hamidi, Azadi, & Rafiei, 2008). On the one hand, the preparation of synthetic polymers is often well understood and controlled, leading to "smart" materials with finely tuned characteristics. However, these polymers cannot be guaranteed for innocuousness, because of potential reactants remaining from their synthesis or products resulting from the polymer enteric degradation (Goddard & Hotchkiss, 2007). Moreover, these systems rely on the use of non-renewable resources. Biopolymers also exhibit disadvantages that must be overcome for delivery applications (e.g. variability of their physicochemical characteristics depending on their source). However, biopolymers that can readily make hydrogels (e.g. chitosan, carrageenan and starch) are well known for their biocompatibility and non-toxicity (Chandra & Rustgi, 1998; Reis & Cunha, 2001; Varshosaz, 2007). In this perspective, starch has been widely studied, after modifications or in combinations with other polymers (Calinescu, Mulhbacher, Nadeau, Fairbrother, & Mateescu, 2005; Elvira, Mano, San Román, & Reis, 2002; Fransén, Björk, & Edsman, 2008; Oechslein, Fricker, & Kissel, 1996; Onofre, Wang, & Mauromoustakos, 2009; Rahmouni et al., 2003; Tuovinen et al., 2004).

In the case of in vivo delivery of bioactive compounds, whether the carriers are pre-hydrated hydrogels or hydrogels formed in situ from dry particles, these systems rely on the capability of the polymer network to swell upon water absorption and eventually to disintegrate, in order to let active compounds be released and diffuse (Peppas & Brannon-Peppas, 2001). This disintegration can also be achieved via digestion of starch in the gastrointestinal tract: swelling and leaching of the loaded particles are here crucial parameters to tune the kinetics of degradation, because they will affect the accessibility of glucan chains to the digestive enzyme α-amylase (Cristina Freire, Fertig, Podczeck, Veiga, & Sousa, 2009). Achieving a wide range of swelling and leaching characteristics can then lead to controlled delivery profiles of target compounds. Thus, this study aims to show that microparticles having potential for simple delivery systems can be prepared from starch only, by taking advantage of starch molecular properties and characteristics.

Starch is composed of amylopectin and amylose, two high molecular-weight, polydisperse (1,4)-α-D-glucans. Amylopectin is highly branched through (1,6)-α linkages (M_w ~5×10^7–5×10^8, average chain length ~20–30 units) and soluble in water as an isolated polymer (as opposed to native state in granular form), and amylose is linear or slightly branched (M_w ~10^5–10^6, average chain length ~10^2–10^3 units), nearly insoluble in water as an isolated

* Corresponding author. Tel.: +1 765 494 6317; fax: +1 765 494 7953.
E-mail address: yao1@purdue.edu (Y. Yao).
[1] Present address: PepsiCo Global R&D, 617 W Main Street, Barrington, IL 60010, United States.

0144-8617/$ – see front matter © 2013 Elsevier Ltd. All rights reserved.
http://dx.doi.org/10.1016/j.carbpol.2013.11.031

polymer (as opposed to native state in granular form) (Calvert, 1997; Smith & Denyer, 2003). The structure–function relationships of amylose and amylopectin and their interactions in starch networks are well understood (BeMiller, 2007, chap. 6). Among other features, amylopectin and amylose chains are able to form double helices which may in turn associate to form crystallites. In general, native starch is isolated under the form of semi-crystalline granules where amylopectin is mainly responsible for crystallinity (Calvert, 1997). When heated in presence of water, starch granules disrupt and polymers leach out to form a three-dimensional network that turns into a gel upon cooling. Cohesiveness of this gel is provided by the double helices formed by associated glucan chains (junction zones) and amylopectin is mainly responsible for long-range interactions. These associations can reach a further extent until partially recreating crystallinity (Mitchell, 2005; Smith & Denyer, 2003). This process, called retrogradation, involves amylose in the first stages and amylopectin over a longer time-scale and in a lesser extent. From the sole standpoint of starch characteristics, crystallinity of retrograded starch depends on factors such as molecular weight and chain lengths of both amylose and amylopectin and branching patterns of amylopectin (Gidley, 1989; Gidley & Bulpin, 1989; Mua and Jackson, 1997a, 1997b). However, water content (interfering with hydrogen bonding of glucan chains) and temperature profile (modifying kinetics of associations) also play major roles in network formation and retrogradation (Gidley & Bulpin, 1989; Kim, Kim, & Shin, 1997; Robin, Mérinat, Simon, & Lehmann, 2008).

In this study, molecular weight, branching degree, amylose/amylopectin ratio and crystallinity of starch polymer were considered as essential parameters to characterize starch microparticles designed as potential delivery systems, all of which affect the swelling and leaching behaviors of starch-based retrograded particules.

Indeed, weight average molecular weight (M_w) and polydispersity are two obvious parameters characterizing starch at the molecular level. Considering polydispersity allows taking into account the distribution of molecular masses in two given starches that would have the same weight average molecular weight (Gidley et al., 2010). It gives a realistic idea of what the starch network is composed of (a blend of extremely long and extremely short chains vs. a homogeneous blend of medium length chains, for example).

Apparent amylose content and crystallinity were chosen as potential parameter controlling swelling and leaching properties of the particles. Indeed, amylose chains are known to interact rapidly by forming double helices referred as junction zones in these networks. Amylopectin chains are also known to exhibit similar interactions, but these latter need a much longer period of time to occur, which may be over a week-long storage period (Gidley, 1989; Gidley & Bulpin, 1989; Mua and Jackson, 1997a, 1997b). These double helices can be packed and arranged in crystalline structures, which represent a higher degree of order compared to junction zones and are quantified by the crystallinity parameter. Apparent amylose content and crystallinity could a priori be considered respectively as indirect and direct markers of the strength of the three-dimensional network created by amylose and amylopectin (Gidley et al., 2010; Rindlav, Hulleman, & Gatenholm, 1997; Rindlav-Westling, Stading, Hermansson, & Gatenholm, 1998; Rindlav-Westling, Stading, & Gatenholm, 2002).

In this study, it was decided not to choose the branching degree as a pertinent parameter. The branching degree would have allowed differentiating the ordered structure occurring from amylose or amylopectin (Reis & Cunha, 2001). However, this differentiation appeared to be already considered in our study, since debranching (i.e. the reduction of branching degree) directly leads to increased apparent amylose content. In addition, lightly branched amylopectin molecules (after debranching treatment) could also be involved in junction zones or crystalline patterns and could participate to the strengthening of the starch network, affecting the swelling and leaching properties of the particles. These effects are taken into account by the measurement of apparent amylose content and crystallinity, as well as M_w and polydispersity, and the characterization of branching degree could be considered redundant in this perspective.

Subsequently, this study aims to: (1) provide a practical platform for manipulating the swelling and leaching properties of "starch-only" microparticles, and (2) reveal the impact of amylose and amylopectin on the specific properties of starch particulates as potential delivery agents. To achieve this aim, microparticles were made by water-in-oil emulsion from starches that were specifically degraded and debranched. Their swelling and leaching properties in water were characterized, and these two parameters were modeled according to molecular parameters of starch, including molecular weight and polydispersity, amylose content, and crystallinity.

2. Experimental

2.1. Materials

Normal corn starch (NCS, 24.8% amylose), high amylose corn starch (HACS, 74.1% amylose) and waxy corn starch (WCS, 0% amylose) were provided by Cargill Inc. (Minneapolis, MN). All chemicals were purchased from VWR International (Radnor, PA) except for those indicated otherwise.

2.2. Starch modification

2.2.1. Acid hydrolysis

A 30% (w/w on dry starch basis) slurry was made by dispersing starch in 0.6 M hydrochloric acid. The slurry was placed in an oscillating water bath at 50 °C and agitated at 90 rpm over 4, 8 or 16 h. After acid treatment, the slurry was neutralized with 1.0 M sodium hydroxide and centrifuged at 3200 × *g* and 4 °C for 10 min (Allegra 6KR centrifuge, Beckman Coulter, Brea, CA). The starch recovered was then washed three times with de-ionized water and recovered each time by centrifugation (3200 × *g*, 4 °C, 10 min). The recovered starch was then dried overnight in a ventilated oven (FED53 with R3.1 controller, Binder, Bohemia, NY) at 55 °C. In further description of the materials, a 0-h acid treatment means that starch did not undergo the acidic treatment but was dried overnight along the samples with acid treatment.

2.2.2. Debranching

A 5% (w/w on dry starch basis) slurry was made by dispersing starch in a 200 mM sodium acetate aqueous solution (pH 5.0), and autoclaved at 121 °C for 10 min. The gel obtained was cooled to 40 °C in an agitated water bath (90 rpm, 40 °C) and pullulanase (P5420 from *Klebsiella pneumoniae*, Sigma–Aldrich, St. Louis, MO) was added (2.0%, w/w on dry starch basis). Debranching was performed for 9, 18 or 36 h in a water bath. At the end of the treatment, the starch dispersion was placed for 10 min in a boiling water bath to inactivate the enzyme. Starch was then precipitated with ethanol, recovered by centrifugation (3200 × *g*, 4 °C, 10 min), washed three times with ethanol and recovered each time by centrifugation (3200 × *g*, 4 °C, 10 min). The recovered starch was then dried overnight in an oven with air-circulation at 55 °C. In further description of the materials, a 0-h debranching refers to starch that did not undergo the pullulanase treatment but was autoclaved, placed in a boiling water bath, precipitated with ethanol, washed with ethanol and dried overnight like debranched starches.

Materials are subsequently coded as follows: "type of starch-acid treatment time-debranching time". For example, high amylose

corn starch acid treated for 4 h and not debranched will be coded "HACS-4-0".

2.3. Starch microparticles formation

A 17.5% (w/w on dry starch basis) suspension was made by dispersing treated starch in de-ionized water and subsequent autoclave at 130 °C for 10 min. At the same time, a mixture of 30 mL mineral oil and 2 mL of sorbitan sesquiester emulsifier (Span 83, Sigma–Aldrich, St Louis, MO) was heated to 90–95 °C. As soon as starch autoclaving was completed, 8 mL of the hot starch solution was homogenized with the oil-Span mixture, at 24,000 rpm (T18 Ultra Turrax homogenizer, IKA, Wilmington, NC) for 1 min (temperature dropped to ~40 °C during this process). The suspension was then placed at 4 °C for 24 h to allow starch to retrograde. Starch microparticles were recovered by filtration, washed three times with hexane and three times with ethanol and dried overnight in a ventilated oven at 55 °C. After drying, the microparticles were conditioned at 53% relative humidity (over a saturated $Mg(NO_3)_2$ solution at 23 °C) until they reached a constant weight (in about a week).

2.4. Apparent amylose content determination

Apparent amylose content was assessed with the iodine binding method as described in details in the Method E2.3.5 of Current Protocols in Food Analytical Chemistry (Hoover & Ratnayake, 2001). Briefly, iodine and amylose form an inclusion complex that has a maximum absorbance around 600–620 nm. Thus, it is possible to create a calibration curve of absorbance at 600 nm as a function of amylose content with standardized mixtures of pure amylose and pure amylopectin. In this study, we used 5-point calibration curve, using 0, 25, 50, 75 and 100% amylose (respectively, 100, 75, 50, 25 and 0% amylopectin), with defatted amylose from potato (Sigma–Aldrich, St. Louis, MO) and defatted amylopectin from maize (Sigma–Aldrich, St. Louis, MO). Then, starch samples made in this study were complexed with iodine, their absorbance read at 600 nm and their apparent amylose content inferred from the calibration curve.

2.5. Particle size measurement

Particle size profile was measured by light scattering with a Malvern Mastersizer 2000 instrument (Malvern, Worcestershire, UK) using a He/Ne laser at 633 nm and an electroluminescent diode at 466 nm. Laser alignment was performed in 100% isopropanol ($n = 1.3776$) and samples were suspended in isopropanol (1%, w/w), at room temperature. Particle size distribution was obtained from data collected every 5 s over 2 min at room temperature, making each particle size distribution the average of 24 measurements.

2.6. Crystallinity of microparticles

About 500 mg of starch sample was packed in an aluminum holder and mounted on a Philips PW3710 diffractometer interfaced with Automated Powder Diffraction (APD) software. Ni-filtered Cu Kα radiation ($\lambda = 1.5418$ Å) was used, and the tube was operated at 40 kV and 25 mA. The intensity data were collected at room temperature at 0.01° intervals in the 2θ range 10–38°, and the time spent at each step was 4 s. The patterns were smoothed for further analysis by the PC-APD (version 3.6) software, and such a process resulted in 695 data points for the entire pattern. As the X-ray analysis reflects the average of multiple scans for a sample and shows highly reproducible results, a single test was conducted for each sample. In order to calculate the crystallinity of each starch sample, initially around 450 data points in the nonpeak regions were selected as background intensities. A ninth order polynomial was fitted using the Origin 7.5 Evaluation version, generating the background profile. Further, the cubic spline interpolation methodology was used for estimating the background intensity at each measured diffraction angle (2θ) (Subbotin). The background profile was scaled such that it abuts the semi crystalline pattern. The percentage of crystallinity was calculated as follows:

$$\%\,\text{crystallinity} = \frac{(\text{total area} - \text{background profile area})}{\text{total area}} \times 100\%$$

2.7. Swelling power, percentage of leaching and characterization of leached materials of microparticles

About 0.100 g of starch microparticles (equilibrated at 53% relative humidity) accurately weighed (weight w_1) was soaked in 1.0 mL de-ionized water (weight w_2) for 30 min at 23 °C, in a 2 mL microcentrifuge tube. The tube and its content were centrifuged at 17,500 × g for 2 min (Microfuge 22R, Beckman Coulter, Brea, CA). The precipitate and the supernatant were weighed (weights w_3 and w_4, respectively). They were separately dried overnight in a ventilated oven at 55 °C. The two subsequent fractions, dry precipitate and dried supernatant, were weighed again (weights w_5 and w_6, respectively).

A mass-balance control was made to check that $w_1 + w_2 = w_3 + w_4$, with a tolerance of 5%.

The swelling power of the material was then calculated as:

$$\text{Swelling power} = \frac{w_3}{w_5}.$$

The percentage of leaching was calculated as:

$$\text{Percentage of leaching} = \frac{w_6}{w_1} \times 100\%.$$

Swelling power and percentage of leaching measurement methods are summarized in Fig. 1.

The dried supernatant (weight w_6), defined as leached material, was then characterized using high performance size exclusion chromatography system coupled with a multi-angle laser scattering detector and a differential refractive index detector (HPSEC-MALS-RI) according to the same protocol as in 2.8 to determine its M_w and polydispersity.

2.8. Molecular weight and polydispersity measurement

A 1% (w/w on dry starch basis) suspension was made by dispersing dry samples in 100% HPLC grade DMSO and heated for 10 min in a boiling water bath. The subsequent clear solution was centrifuged for 5 min at 17,500 × g and 4 °C (Microfuge 22R, Beckman Coulter, Brea, CA), the supernatant was decanted, and filtered through a 0.22 μm syringe-filter. Twenty microliters of this solution were then injected on an HPSEC-MALS-RI system. This system was composed of a Waters HPLC 515 pump (Waters, Milford, MA), an Agilent PLGel 20 μm guard column, an Agilent PLGel 20 μm Mixed A column (Agilent, Lexington, MA), a Wyatt Optilab T-rEX RI detector coupled with a Wyatt DAWN HELEOS II multi-angle laser scattering detector (Wyatt, Santa Barbara, CA). HPLC grade DMSO was used as mobile phase at 0.3 mL/min. The signal analyzed by the two detectors was normalized using a pullulan standards ($M_w = 50{,}000$, polydispersity = 1.06) provided by Sigma (Saint-Louis, MO). Data was acquired and processed by Wyatt's software ASTRA V. A dn/dc value of 0.0659 L g^{-1} was used (Chakraborty, Sahoo, Teraoka, & Gross, 2005; Yokoyama, Renner-Nantz, & Shoemaker, 1998) and a second-order Berry formalism was used to calculate the molecular

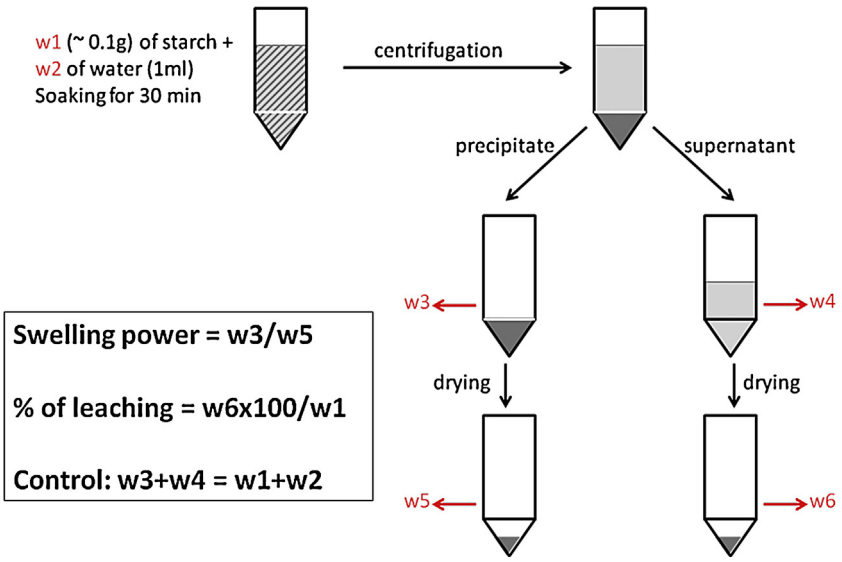

Fig. 1. Schematic summary of swelling power and percentage of leaching measurement methods.

weight of starch samples. ASTRA V software estimated by calculation the number-average molecular weight M_n of the polymers, and thus calculated their polydispersity index as M_w/M_n. Finally, from the standpoint of calculations and statistical treatment, it was chosen to use the variable Log M_w instead of M_w, for practical reasons, but it would not prevent any interpretation directly related to the physical parameter M_w.

2.9. Statistical treatment and response surface models

Apparent amylose content, swelling power and percentage of leaching determinations were all performed in triplicate. Values are given as mean ± confidence interval ($p < 0.05$).

The four variables measured and used in this study (M_w, polydispersity and apparent amylose of the microparticles starch, and crystallinity of these microparticles) were used to model this output variable by response surface method. Briefly, if V is an output variable whose variations are due to input variables W, X, Y and Z, experimental data consisting of quintuplets (V; W; X; Y; Z) were used to compute a second order equation (representing a surface) by least square regression and to provide a model $V = f(W, X, Y, Z)$. The model obtained is called "full model" as it contains linear and quadratic effects of the variables, as well as interactions between these variables. A regression coefficient R^2 for the model is calculated, providing an estimate of the level of data variance explained by the model itself. Provided that R^2 has a satisfying value, the model $V = f(W, X, Y, Z)$ can be interpolated: one would know easily what values of input variables W, X, Y and Z would lead to a desired value for output variable V, within the limits of the experimental data provided initially.

In this study, the response surface method was computed using SYSTAT 12 (SYSTAT Software Inc., Chicago, IL).

3. Results and discussion

The goal of this study was to understand what were the key parameters driving the four output variables studied (swelling power of microparticles, amount of material leached out in water, M_w and polydispersity of material leached out) in order to tailor starches according to desirable properties for future applications of microparticles as potential delivery systems. Among these parameters, as stated in the introduction, we focused on easily accessible molecular and macroscopic characteristics: weight-average molecular weight (M_w), estimated polydispersity and apparent amylose content of starch in microparticles and crystallinity of the microparticles. By obtaining estimate models of swelling power and leaching properties as functions of these parameters and by knowing the respective intensities of their effects, we were able to interpret more accurately the physical phenomena underlying the swelling and the leaching of starch microparticles into water.

Finally, absolute values of M_w must be considered with care. Indeed, there is an ongoing debate on the measurement of M_w of starch and starch components: SEC-MALS-RI system seems to be a satisfactory technique to achieve this goal, but some pitfalls remain. For example, amylopectin is thought to breakdown partially during separation in the SEC columns, because of the shear forces it is subjected to in this process, especially when DMSO is used as a mobile phase because of its viscosity, which can lead to an underestimation of M_w; this effect could be avoided by using an aqueous mobile phase due to a much lower viscosity, though it promotes starch intermolecular associations of starch polymers, thus leading to an overestimation of starch M_w (Gidley et al., 2010; Hoang et al., 2008; You & Lim, 2000). However, none of these mobile phases seems fully satisfying (Gilbert et al., 2010), so far, and we can only remind the reader about this fact.

Similar care should be taken about apparent amylose content values. Indeed, its measurement relies on the ability of amylose and amylopectin standard to bind iodine, with the assumption that amylose is a purely linear polymer and amylopectin does not complex with iodine (Herrero-Martínez, Schoenmakers, & Kok, 2004). In fact, it has been proven that amylose exhibits some branching and some longer branches of amylopectin can complex with iodine (Chen & Bergman, 2007; Tester & Karkalas, 1996). Moreover, starch and starch hydrolysis products cannot strictly be divided into two categories, namely amylose and amylopectin: intermediate material (lightly branched low M_w amylopectin or branched high M_w amylose) exist in native starch and subsequently in starch hydrolysis products (Chen & Bergman, 2007). Thus, the calibration curve obtained for apparent amylose content as a function of absorbance at 600 nm and the assessment of starch products against this calibration curve may be taken with caution. However, once again, we can only remind the reader about this fact.

3.1. Characteristics of modified starches and microparticles

Tables 1–3 show the characteristics of starches obtained from NCS (Table 1), HACS (Table 2) and WCS (Table 3), respectively.

We were able to obtain a set of materials with diverse structural parameters. The wide ranging of these parameters would be beneficial to further model studies. Indeed, M_w ranged from 3.6×10^7 for WCS-0-0 to 2.5×10^4 for WCS-16-18, which is consistent with values reported in former studies (Han, BeMiller, Hamaker, & Lim, 2003; Nakajima, Iwasaki, Nabetani, & Watanabe, 1990; Smith & Denyer, 2003). M_w was ranging 2.2×10^7–3.4×10^4, 3.4×10^6–5.1×10^4 and 3.6×10^7–2.5×10^4 for NCS, HACS and WCS-based starches, respectively. These values showed that we obtained a large and continuous range of M_w after acidic and enzymatic treatment of the three kinds of raw starch materials. Although polydispersity values of all the materials are comparable (3.9 ± 1.2 ranging 1.00–9.16, 5.6 ± 1.6 ranging 2.79–9.74 and 4.4 ± 1.1 ranging 1.47–8.60, for NCS, HACS and WCS-based starches, respectively) as well as their degrees of crystallinity (13.1 ± 2.5 ranging 7.63–21.55, 13.5 ± 1.8 ranging 7.99–19.16 and 15.1 ± 3.4 ranging 4.31–22.84, for NCS, HACS and WCS-based starches, respectively), their apparent amylose contents still reflects the composition of the starches they were made from (45.5 ± 8.4 ranging 24.81–79.33, 87.1 ± 5.4 ranging 71.03–99.44 and 15.4 ± 4.2 ranging 2.31–27.89, for NCS, HACS and WCS-based starches, respectively). Let us note that the polydispersity value of sample HACS-8-18 was considered as a statistical outlier, and then discarded from the data set for calculation of the response surface models. Regarding the effect of the treatments these starches have undergone, characteristic patterns can be observed about crystallinity and apparent amylose content that tend to increase with debranching time, up to a point where it undergoes a sharp decrease. It can be hypothesized that, during the first stages of debranching, steric hindrance is lowered in amylopectin and more branched chains are able to participate in the formation of crystallites, especially the longer ones that are in the core of amylopectin molecules. Then, during further stages of debranching, small chains may be released, increasing the amount of amorphous material because of their inability to participate in the formation of these crystallites. However, this measurement does not take into account the amount of junction zone that certainly play a role in the properties of the three-dimensional networks formed by amylopectin and amylose and then in the swelling and leaching properties of these networks.

It is also worth being noted that we obtained wide and continuous ranges of swelling power values (4.1 ± 0.6 ranging 3.00–7.84, 3.5 ± 0.1 ranging 3.12–3.85 and 3.1 ± 0.3 ranging 2.45–4.32, on average for starches made from NCS, HACS and WCS, respectively) and percentages of leaching (16.9 ± 6.3 ranging 1.72–40.12, 5.0 ± 1.4 ranging 2.24–11.11 and 28.5 ± 11.1 ranging 8.11–74.91, on average for NCS, HACS and WCS-based starches, respectively).

Particle size distributions were also determined by light scattering. For all the materials, particle size distributions exhibited similar patterns: the mean particle diameter was 15–20 μm, 90% of the particles diameters were in the range of 5–45 μm, and the diameter of the biggest particles never exceeded 200 μm. Given the homogeneity of the dimensions of all the particles studied, particles size and specific area were considered as non-relevant parameters in order to understand swelling and leaching.

3.2. Percentage of leaching

A surface equation modeling percentage of leaching was generated and the coefficients assigned to its effects are reported in Table 4. R^2 for this model is 0.890 (calculated by the method of least square means), which means that ~89% of the percentage of leaching variance was explained by the model obtained.

Table 1
Characteristics of starches (weight-average molecular weight (M_w), polydispersity, apparent amylose content) and microparticles (swelling power, percentage of leaching, M_w and polydispersity of leached material) derived from acid-treated and debranched normal corn starch. Apparent amylose content, swelling power and percentage of leaching values are given as mean ± SEM ($p < 0.05$, $n = 3$).

Starch type	Acid hydrolysis time (h)	Debranching time (h)	M_w	Polydispersity	Crystallinity(%)	Apparent amylose content (%)	Swelling power	Leaching (%, w/w)	M_w of leached material (Da)	Polydispersity of leached material
NCS	0	0	22,040,000	2.21	7.63	24.81 ± 0.44	7.84 ± 0.15	1.72 ± 0.02	50,550	1.09
NCS	0	9	1,972,000	5.30	14.11	61.38 ± 1.90	3.84 ± 0.07	3.62 ± 0.12	219,900	4.12
NCS	0	18	303,800	3.99	19.31	79.33 ± 1.15	4.05 ± 0.62	4.18 ± 0.68	248,600	32.27
NCS	0	36	47,340	7.86	17.95	61.92 ± 1.59	3.51 ± 0.08	4.50 ± 0.15	290,100	5.21
NCS	4	0	51,860	1.01	8.47	30.44 ± 0.63	4.97 ± 0.04	20.64 ± 0.96	79,110	12.01
NCS	4	9	286,600	1.99	7.88	37.41 ± 0.84	3.62 ± 0.04	22.51 ± 1.73	364,800	1.86
NCS	4	18	155,500	2.67	10.38	42.90 ± 0.68	4.11 ± 0.20	15.26 ± 2.84	202,300	4.63
NCS	4	36	273,600	5.65	16.84	63.39 ± 0.87	3.66 ± 0.13	8.56 ± 0.62	196,600	8.00
NCS	8	0	121,800	1.71	9.55	32.05 ± 0.47	4.80 ± 0.15	28.33 ± 1.44	43,690	1.00
NCS	8	9	106,500	2.82	7.99	43.30 ± 0.50	4.03 ± 0.23	23.47 ± 0.39	981,300	5.18
NCS	8	18	595,200	1.82	19.88	55.22 ± 0.86	3.36 ± 0.16	9.76 ± 0.11	140,000	9.59
NCS	8	36	34,460	4.46	21.55	66.74 ± 1.26	3.09 ± 0.03	6.27 ± 0.03	209,300	8.96
NCS	16	0	77,120	1.99	9.11	30.57 ± 1.09	4.09 ± 0.08	34.27 ± 1.53	42,760	1.32
NCS	16	9	47,740	1.00	9.51	26.29 ± 0.89	4.10 ± 0.04	40.12 ± 0.81	44,370	5.74
NCS	16	18	308,500	9.16	18.71	45.18 ± 1.48	3.00 ± 0.16	10.65 ± 1.11	100,600	10.28
NCS	16	36	290,800	6.58	10.89	27.76 ± 0.51	4.02 ± 0.12	37.04 ± 1.12	297,500	1.48

Table 2
Characteristics of starches (M_w, polydispersity, apparent amylose content) and microparticles (swelling power, percentage of leaching, M_w and polydispersity of leached material) derived from acid-treated and debranched high amylose corn starch. Apparent amylose content, swelling power and percentage of leaching values are given as mean ± SEM ($p < 0.05$, $n = 3$). Polydispersity value in parentheses was considered as an outlier.

Starch type	Acid hydrolysis time (h)	Debranching time (h)	M_w	Polydispersity	Crystallinity (%)	Apparent amylose content (%)	Swelling power	Leaching (% w/w)	M_w of leached material (Da)	Polydispersity of leached material
HACS	0	0	3,356,000	4.22	8.61	74.11 ± 1.34	3.42 ± 0.17	2.24 ± 0.48	974,200	2.62
HACS	0	9	218,600	4.38	12.96	80.94 ± 1.45	3.59 ± 0.07	2.85 ± 0.34	186,200	4.93
HACS	0	18	315,500	4.48	14.22	82.15 ± 0.55	3.63 ± 0.04	2.57 ± 0.46	222,200	8.59
HACS	0	36	161,900	4.31	16.66	81.75 ± 0.83	3.64 ± 0.03	4.07 ± 0.84	143,600	8.73
HACS	4	0	214,900	3.02	8.50	98.23 ± 1.77	3.75 ± 0.06	4.01 ± 0.50	704,800	1.46
HACS	4	9	111,900	2.79	12.88	99.44 ± 0.56	3.85 ± 0.19	2.74 ± 0.73	43,570	1.00
HACS	4	18	80,930	4.10	13.95	96.48 ± 1.46	3.45 ± 0.13	4.35 ± 0.47	312,900	5.45
HACS	4	36	97,300	4.36	17.59	99.44 ± 0.56	3.29 ± 0.02	3.22 ± 0.22	275,700	5.07
HACS	8	0	104,200	2.86	7.99	88.71 ± 1.78	3.64 ± 0.12	7.35 ± 1.69	173,100	2.29
HACS	8	9	67,680	3.63	12.81	98.81 ± 1.19	3.36 ± 0.08	4.30 ± 0.53	290,400	3.13
HACS	8	18	89,320	(15.18)	14.82	90.45 ± 0.96	3.25 ± 0.03	2.94 ± 0.02	880,600	3.35
HACS	8	36	94,420	8.38	16.83	95.94 ± 1.64	3.29 ± 0.18	3.46 ± 0.76	860,300	4.85
HACS	16	0	50,820	3.83	9.34	77.73 ± 1.68	3.35 ± 0.05	9.41 ± 0.08	107,200	2.20
HACS	16	9	249,200	6.59	10.98	73.04 ± 1.47	3.45 ± 0.33	11.11 ± 1.77	175,600	4.06
HACS	16	18	224,700	9.74	18.05	78.53 ± 0.54	3.12 ± 0.01	5.36 ± 0.23	877,100	5.52
HACS	16	36	137,000	8.45	19.16	71.03 ± 0.54	3.18 ± 0.12	9.49 ± 0.41	528,500	10.50

Table 3
Characteristics of starches (M_w, polydispersity, apparent amylose content) and microparticles (swelling power, percentage of leaching, M_w and polydispersity of leached material) derived from acid thinned and debranched waxy corn starch. Apparent amylose content, swelling power and percentage of leaching values are given as mean ± SEM ($p < 0.05$, $n = 3$).

Starch type	Acid hydrolysis time (h)	Debranching time (h)	M_w	Polydispersity	Crystallinity (%)	Apparent amylose content (%)	Swelling power	Leaching (%, w/w)	M_w of leached material (Da)	Polydispersity of leached material
WCS	0	0	35,510,000	1.16	–	–	–	–	–	–
WCS	0	9	348,100	6.45	12.87	18.65 ± 0.40	2.91 ± 0.06	17.03 ± 1.07	314,000	11.79
WCS	0	18	192,100	6.60	21.65	27.89 ± 1.23	2.68 ± 0.08	15.48 ± 0.38	134,800	10.34
WCS	0	36	237,700	8.60	21.38	25.75 ± 0.29	2.45 ± 0.02	8.11 ± 0.07	165,100	8.67
WCS	4	0	589,200	1.71	6.86	3.78 ± 0.23	4.32 ± 0.90	74.91 ± 10.00	620,500	1.71
WCS	4	9	92,140	3.78	15.61	19.99 ± 0.86	2.82 ± 0.07	22.53 ± 2.36	1,391,000	6.92
WCS	4	18	92,440	7.78	14.57	18.52 ± 0.52	3.22 ± 0.21	27.42 ± 3.92	272,800	4.33
WCS	4	36	30,540	5.25	22.84	17.85 ± 0.15	2.60 ± 0.01	12.50 ± 0.15	341,900	9.45
WCS	8	0	171,300	1.46	4.41	3.38 ± 0.21	4.20 ± 0.30	48.89 ± 7.34	176,600	1.32
WCS	8	9	28,580	3.67	19.69	21.87 ± 1.24	2.72 ± 0.10	14.96 ± 1.11	145,800	3.79
WCS	8	18	29,860	3.86	20.96	23.21 ± 0.71	2.66 ± 0.09	13.10 ± 0.67	80,380	5.86
WCS	8	36	28,160	5.46	21.16	18.79 ± 0.66	2.45 ± 0.02	9.11 ± 0.22	102,100	6.69
WCS	16	0	53,780	1.47	4.31	2.84 ± 0.18	4.26 ± 0.15	73.24 ± 1.68	113,100	3.12
WCS	16	9	70,700	1.86	4.36	2.31 ± 0.12	3.92 ± 0.23	52.19 ± 2.48	169,200	3.19
WCS	16	18	24,790	4.04	16.90	14.63 ± 0.50	2.61 ± 0.05	14.41 ± 0.22	313,200	8.96
WCS	16	36	27,570	3.90	19.29	12.62 ± 0.56	2.81 ± 0.07	23.97 ± 0.74	288,000	6.65

Table 4
Coefficient of response surface model for percentage of leaching and swelling power, using Log M_w, crystallinity, polydispersity and amylose content as prominent effect.

Effect	% Leaching modeling coefficients	Swelling power modeling coefficients
Constant	−173.445	17.97
Log M_w	92.783	−5.644
Polydispersity	−4.979	0.118
Crystallinity	−1.964	−0.089
Apparent amylose content	−0.74	0.05
Log M_w × Log M_w	−8.462	0.598
Polydispersity × polydispersity	0.211	0.013
Crystallinity × crystallinity	0.08	−0.006
Apparent amylose content × apparent amylose content	0.004	0
Log M_w × polydispersity	0.874	−0.094
Polydispersity × crystallinity	−0.236	0.012
Polydispersity × apparent amylose content	0.03	−0.001
Log M_w × crystallinity	−0.208	0.016
Crystallinity × apparent amylose content	0.017	0.001
Log M_w × apparent amylose content	−0.074	−0.008
	% Leaching model: R^2 = 0.890	Swelling power: R^2 = 0.861

The analysis of variance gave *p*-values for the model as follows: regression $p < 0.0005$, linear $p < 0.0005$, quadratic $p < 0.0005$, interactions $p < 0.086$. It can also be noted that the four main effects are Log M_w, Log M_w × Log M_w, polydispersity and crystallinity, by order of decreasing importance, and that they all have negative effects on the percentage of leaching (percentage of leaching increases when they decrease, all other parameters remaining constant), at the exception of Log M_w (percentage of leaching increases when Log M_w increases). On the other hand, the quadratic (except for Log M_w × Log M_w) and interaction effects (crystallinity × crystallinity, crystallinity × amylose content, crystallinity × polydispersity, etc.) have minor influence in the model.

In line with usual observations on starch materials, a high amount of amylose and a high crystallinity tend to decrease the amount of starchy material leaching out in water. This effect is clearly shown by Fig. 2(d) (percentage of leaching as a function of amylose content and crystallinity) and also by Fig. 2(a) and (b). It was also expected that the microparticles, if considered as a three-dimensional polymeric network, would be characterized by their mesh. A greater number of associations of the polymer chains composing this network would lead to a tighter network less able to let small residues go out of this mesh. Then, it makes sense that a higher crystallinity and amylose content are conditions for obtaining this kind of tighter network, given the ability of amylose chains to associate in junction zones. The effect of polydispersity is less clear. There is no obvious explanation about the fact that a greater polydispersity would prevent material to leach out from the particles. Actually, Fig. 2(a) and (b) show that polydispersity have opposite effects on leaching depending on the amylose content. Indeed, at higher amylose content and lower crystallinity, higher polydispersity leads to higher leaching; at lower amylose content, higher polydispersity leads to lower leaching. At least, we can hypothesize that when the microparticles are formed and allowed to retrograde, the short polymer chains are more mobile than the longer ones and may contribute to forming associations more homogeneously throughout the network. It is also interesting to note that M_w is a significant parameter for modeling the percentage of leaching. Indeed, Fig. 2(c) and (f) clearly show that the lower the M_w, the higher the amount of leaching material. Fig. 2(e) similarly show the synergy between crystallinity and M_w: lower crystallinity and lower M_w leading to sharp increase in amount of leached material. Finally, Fig. 2(d) shows that as expected, at high amylose content, leaching remains almost constantly low while it increases at lower amylose content, this increase being even more dramatic at lower crystallinity. Overall, prolonged acid hydrolysis and debranching leading to a significant decrease in M_w tend to increase to the solubility of starch polymers and thus their leaching out of the microparticles. However, even at reduced M_w, if amylose content is high enough to promote the formation of a consistent three-dimensional network through retrogradation and junction zones, leaching can be limited. The importance of this network is highlighted by the impact of polydispersity on the particles leaching properties: at low crystallinity, leaching increases sharply with decreasing polydispersity, while at high crystallinity, polydispersity have a minor effect on leaching, suggesting that starch polymers with widely distributed M_w (high polydispersity) can be retained by the formation of a highly retrograded, physically cross-linked network.

3.3. Leached out materials

We attempted to model the M_w and the polydispersity of the materials leached out in water from the microparticles, but response surface model showed no evidence of strong effects as for polydispersity, crystallinity, amylose content or M_w of the starting material. Several attempts of modeling these effects lead to surface equations with R^2 not higher than 0.49. This means that not more than 49% the variations of M_w and polydispersity of the materials leached out could be explained by the parameters we considered in this study.

3.4. Swelling power

Finally, a surface equation modeling swelling power was generated and the coefficients assigned to its effects are reported in Table 4. R^2 for this model is 0.861, which means that ~86% of the swelling power variance was explained by the model obtained. The analysis of variance gave *p*-values for the model as follows: regression $p < 0.0005$, linear $p < 0.0005$, quadratic $p < 0.0005$, interactions $p < 0.011$. Once again, this model can be considered as fairly satisfying. It can also be noted that the main effect is by far Log M_w, followed by Log M_w × Log M_w, polydispersity, crystallinity and Log M_w × polydispersity, by order of decreasing importance. Moreover, the other quadratic and interaction effects have minor influence on the model. The coefficient of Log M_w is about 10 times higher than the coefficient of the second most important effect, Log M_w × Log M_w, in absolute value, and they have opposite signs. Thus, when Log M_w (and then M_w) increases, the swelling power decreases down to a point where the variable Log M_w × Log M_w becomes about 10 times as high as Log M_w. At this point and for higher values of Log M_w, Log M_w × Log M_w is prominent and the swelling power increases. This second-order polynomial variation with Log M_w explains the shapes of the surfaces plotting Swelling power as a function of Log M_w shown in Fig. 3, where a saddle point

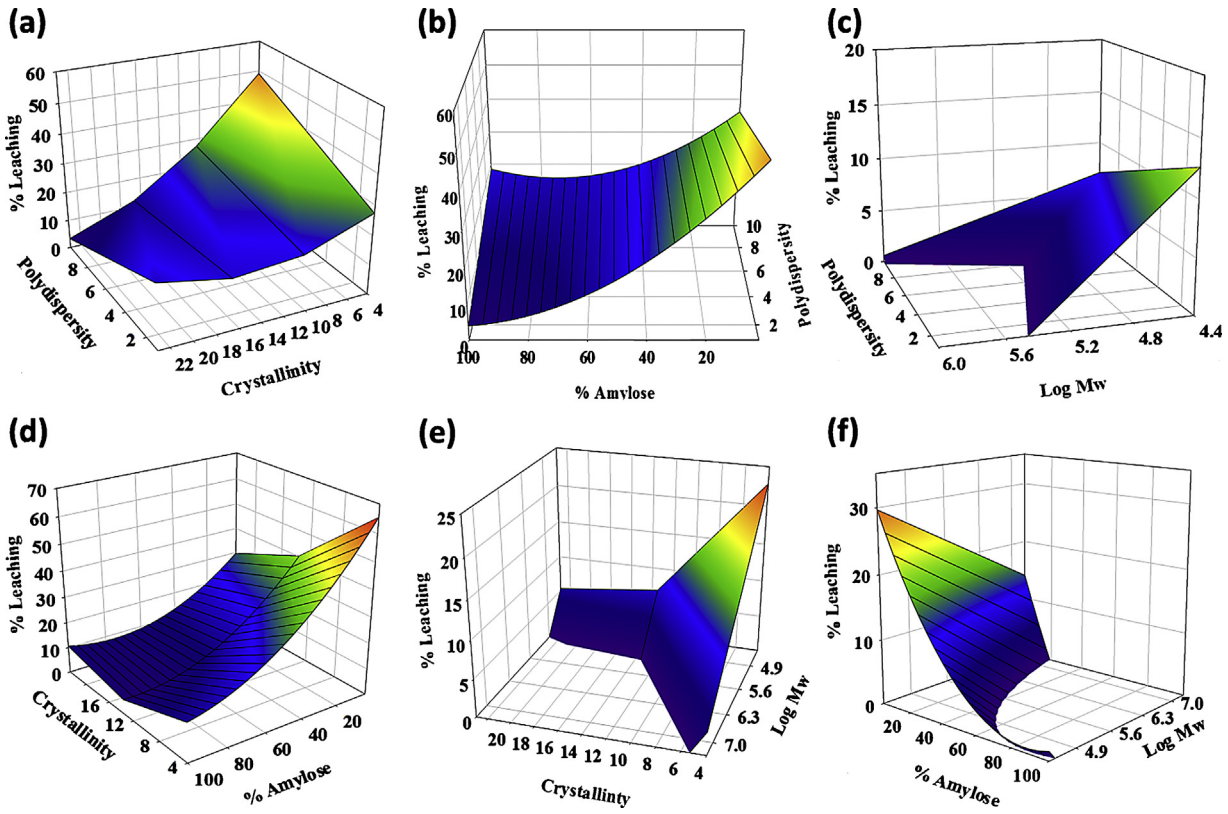

Fig. 2. Surface plot of modeled percentage of leaching as a function of crystallinity, amylose content, polydispersity and Log M_w. When not plotted, variables were fixed at the following values: crystallinity = 13.9%, amylose content = 49.1%, polydispersity = 4.4 and Log M_w = 5.2 (their average value over the population of samples studied).

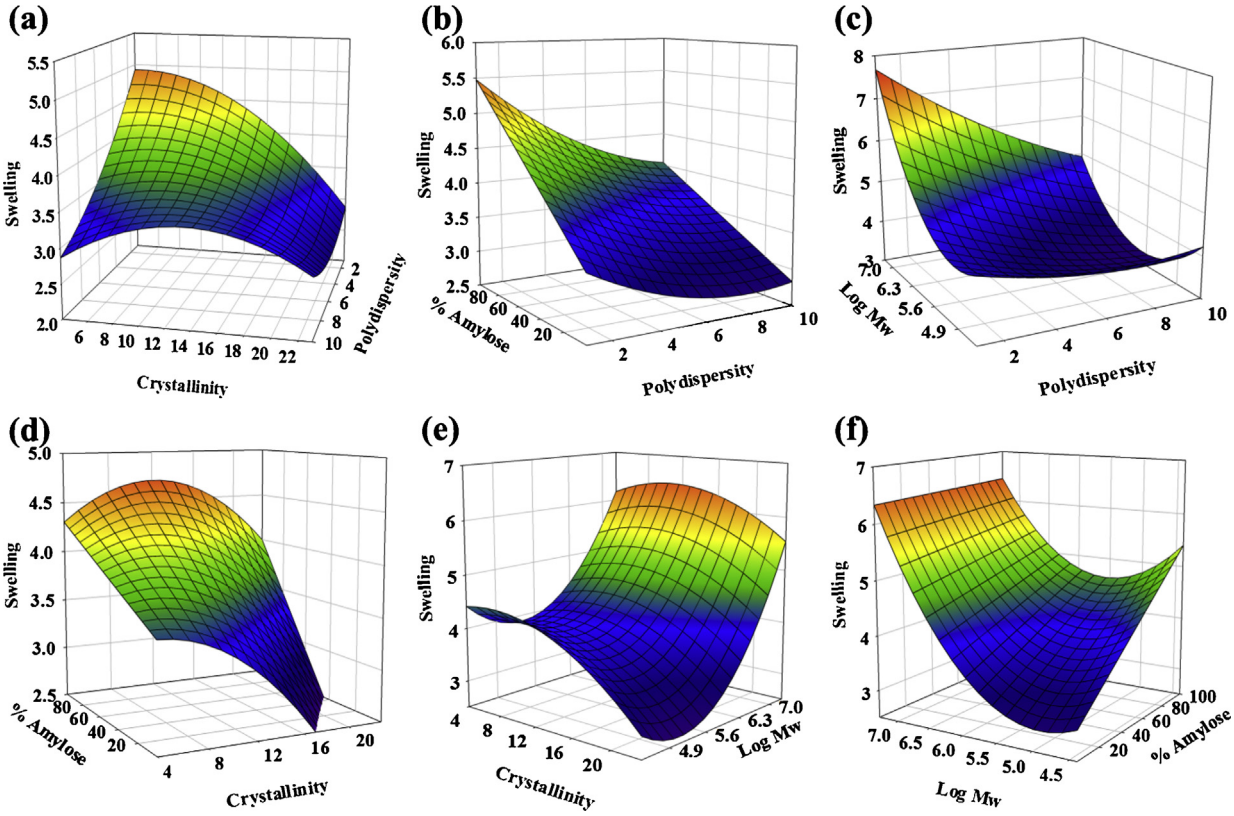

Fig. 3. Surface plot of modeled swelling power as a function of crystallinity, amylose content, polydispersity and Log M_w. When not plotted, variables were fixed at the following values: crystallinity = 13.9%, amylose content = 49.1%, polydispersity = 4.4 and Log M_w = 5.2 (their average value over the population of samples studied).

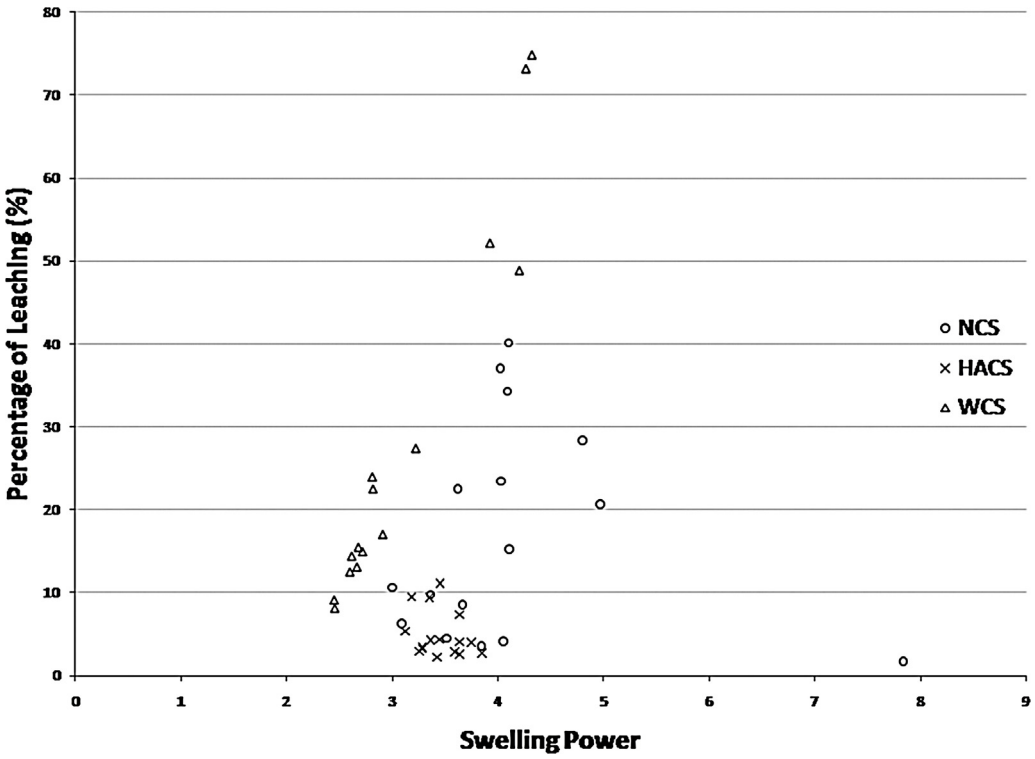

Fig. 4. Percentage of leaching vs. swelling power from samples based on NCS, HACS and WCS.

and a valley can be observed along the Log M_w axes. In that respect, swelling power reaches a minimum for $M_w \sim 10^{5.5}$ and an absolute maximum for the highest values of M_w, as shown in Fig. 3(c), (e) and (f). Generally, as shown in Fig. 3(a), (d) and (e), maximum swelling is reached with crystallinity < 14% (where crystallinity plateaus or reaches a maximum). Swelling power is proportional to amylose content and inversely proportional to polydispersity, as suggested by the response surface factors and Fig. 3(a)–(f). This can be related again to the characteristics of the three-dimensional starch network. It has been shown (Follain, Joly, Dole, & Bliard, 2005; Rindlav et al., 1997; Rindlav-Westling et al., 2002, 1998) that network composed of high molecular weight materials tends to be more flexible and have potentially more inter-chain space to absorb and retain water, without disruption of the network. On the other hand, networks composed of low M_w elements would tend to disrupt more easily in presence of water. Indeed, in the absence of very long chains crossing throughout the whole network and keeping it locked, clusters of the network could be disrupted and leave space for water to come in, water being known to play the role of a plasticizer in this type of network (Follain et al., 2005). As noted previously, swelling power plateaus or reaches a maximum for crystallinity of ~14% and below. This means that swelling power can be kept constant or low for the lowest and the highest values of crystallinity. This could be related to the previous explanation, about the disruption of network clusters: a high crystallinity throughout the network will prevent this latter from swelling, because starch crystallites have very limited flexibility and can hold a very limited amount of water. However, if crystallinity decreases, the material consists in higher amount of amorphous starch and simple junction zones (as opposed to crystallites that are organized and packed double helices). Then, water could be absorbed in higher quantities, leading to disruptions of the network homogeneity, and a higher swelling power. On the other hand, there is no obvious explanation regarding the low swelling power obtained from low crystallinity values. In this perspective, retrogradation was promoted in order to promote potential crystallization. However, with the same types of starches, promoting the formation of amorphous materials could be helpful to understand and clarify some of the effects underlying the absorption of water in starch networks. Indeed, methods using very quick drying of starch particles and immobilization of the polymer chains without time for retrogradation could be helpful, and spray drying could be a good candidate for that. Finally, it is worth noting that amylose content did not appear to be an important factor for modeling the swelling power. This could mean that when retrogradation is highly promoted, amylose and amylopectin do not have radically different behavior regarding water absorption. In both cases, inter-chain space is notably reduced and water uptake is decreased. Once again, promoting the formation of amorphous material could lead to differentiation between these two polymers and different outcomes regarding materials properties.

3.5. Percentage of leaching vs. swelling power relationship

No obvious relationship was found between swelling power and leaching of the starch materials ($R^2 = 0.197$ for linear correlation), although straightforward observations can be made from the mapping of the materials according to their percentage of leaching vs. swelling power (Fig. 4). Microparticles made from WCS tend to populate the low-swelling area of this scatter plot over a wide range of leaching values. In contrast, materials made from HACS tend to concentrate in the low-leaching-low-swelling part of this plot, while materials made from NCS are more widespread. Additionally, except NCS 0-0, no material exhibit clearly high-swelling-low-leaching properties. However, we can speculate that appropriate formulations of different materials prepared in this study could reach this goal, and this work would deserve further attention.

Finally, it must be noted that microparticles were formed by a unique water-in-oil emulsion technique. To our knowledge, it is the first time that such a technique is used with simple starch to form self-holding particles without need of chemical cross-linking. This extremely simple technique could easily be transposed to larger

scales, even with food grade ingredients such as edible oils. Some of its obvious advantages are: the innocuousness of the chemicals used (in our procedure, hexane used can be easily replaced by other cleaning methods), the innocuousness of the material itself (only starch, physically cross-linked) and the simplicity of the process (a batch or counter-current process can be expected for larger scale production). Moreover, numerous chemical engineering methods are already known to tune this process, in order to create various materials adapted to each specific use (different swelling/leaching properties, different particle size), and genetic engineering of starch sources may also help limiting the need for chemically modifying the starch.

4. Conclusion

This study is aimed at providing both a theoretical and a practical framework for the use of starch in applications related to the potential encapsulation and release of active ingredients, under the form of microparticles. We believe this study has shown that for numerous applications, starch itself does not require chemical modifications, neither sophisticated processes. However, this could not be achieved without understanding further what drives the behavior of these starch microparticles. Thus, swelling power and percentage of leaching of the microparticles were correlated to simple molecular characteristics of the starch, and these later can be controlled to finely tune the macroscopic properties of the material. Further work is then needed to correlate the properties observed here with actual controlled release of bioactive compounds.

References

BeMiller, J. N. (2007). Starches, modified starches, and other starch products. In J. N. BeMiller (Ed.), *Carbohydrate chemistry for food scientists* (pp. 173–223). St. Paul, MN: AACC International Press.

Calinescu, C., Mulhbacher, J., Nadeau, E., Fairbrother, J. M., & Mateescu, M. A. (2005). Carboxymethyl high amylose starch (CM-HAS) as excipient for *Escherichia coli* oral formulations. *European Journal of Pharmaceutics and Biopharmaceutics*, *60*(1), 53–60.

Calvert, P. (1997). Biopolymers: The structure of starch. *Nature*, *389*(6649), 338–339.

Chakraborty, S., Sahoo, B., Teraoka, I., & Gross, R. A. (2005). Solution properties of starch nanoparticles in water and DMSO as studied by dynamic light scattering. *Carbohydrate Polymers*, *60*(4), 475–481.

Chandra, R., & Rustgi, R. (1998). Biodegradable polymers. *Progress in Polymer Science (Oxford)*, *23*(7), 1273–1335.

Chen, M. H., & Bergman, C. J. (2007). Method for determining the amylose content, molecular weights, and weight- and molar-based distributions of degree of polymerization of amylose and fine-structure of amylopectin. *Carbohydrate Polymers*, *69*(3), 562–578.

Cristina Freire, A., Fertig, C. C., Podczeck, F., Veiga, F., & Sousa, J. (2009). Starch-based coatings for colon-specific drug delivery. Part I: The influence of heat treatment on the physico-chemical properties of high amylose maize starches. *European Journal of Pharmaceutics and Biopharmaceutics*, *72*(3), 574–586.

Elvira, C., Mano, J. F., San Román, J., & Reis, R. L. (2002). Starch-based biodegradable hydrogels with potential biomedical applications as drug delivery systems. *Biomaterials*, *23*(9), 1955–1966.

Follain, N., Joly, C., Dole, P., & Bliard, C. (2005). Mechanical properties of starch-based materials. I. Short review and complementary experimental analysis. *Journal of Applied Polymer Science*, *97*(5), 1783–1794.

Fransén, N., Björk, E., & Edsman, K. (2008). Changes in the mucoadhesion of powder formulations after drug application investigated with a simplified method. *Journal of Pharmaceutical Sciences*, *97*(9), 3855–3864.

Gidley, M. J. (1989). Molecular mechanisms underlying amylose aggregation and gelation. *Macromolecules*, *22*(1), 351–358.

Gidley, M. J., & Bulpin, P. V. (1989). Aggregation of amylose in aqueous systems: The effect of chain length on phase behavior and aggregation kinetics. *Macromolecules*, *22*(1), 341–346.

Gidley, M. J., Hanashiro, I., Hani, N. M., Hill, S. E., Huber, A., Jane, J. L., et al. (2010). Reliable measurements of the size distributions of starch molecules in solution: Current dilemmas and recommendations. *Carbohydrate Polymers*, *79*(2), 255–261.

Gilbert, R. G., Gldley, M. J., Hill, S., Kilz, P., Rolland-Sabaté, A., Stevenson, D. G., et al. (2010). Characterizing the size and molecular weight distribution of starch: Why it is important and why it is hard. *Cereal Foods World*, *55*(3), 139–143.

Goddard, J. M., & Hotchkiss, J. H. (2007). Polymer surface modification for the attachment of bioactive compounds. *Progress in Polymer Science (Oxford)*, *32*(7), 698–725.

Hamidi, M., Azadi, A., & Rafiei, P. (2008). Hydrogel nanoparticles in drug delivery. *Advanced Drug Delivery Reviews*, *60*(15), 1638–1649.

Han, J. A., BeMiller, J. N., Hamaker, B., & Lim, S. T. (2003). Structural changes of debranched corn starch by aqueous heating and stirring. *Cereal Chemistry*, *80*(3), 323–328.

Herrero-Martínez, J. M., Schoenmakers, P. J., & Kok, W. T. (2004). Determination of the amylose-amylopectin ratio of starches by iodine-affinity capillary electrophoresis. *Journal of Chromatography A*, *1053*(1–2), 227–234 (special issue).

Hoang, N. L., Landolfi, A., Kravchuk, A., Girard, E., Peate, J., Hernandez, J. M., et al. (2008). Toward a full characterization of native starch: Separation and detection by size-exclusion chromatography. *Journal of Chromatography A*, *1205*(1–2), 60–70.

Hoover, R., & Ratnayake, W. S. (2001). *Determination of total amylose content of starch. Current protocols in food analytical chemistry*. John Wiley & Sons, Inc.

Kim, J. O., Kim, W. S., & Shin, M. S. (1997). A comparative study on retrogradation of rice starch gels by DSC, X-ray and α-amylase methods. *Staerke[nl]Starch*, *49*(2), 71–75.

Mitchell, G. (2005). Carbohydrates | starch. In W. Paul, T. Alan, & P. Colin (Eds.), *Encyclopedia of analytical science* (2nd ed., pp. 440–447). Oxford: Elsevier.

Mua, J. P., & Jackson, D. S. (1997a). Fine structure of corn amylose and amylopectin fractions with various molecular weights. *Journal of Agricultural and Food Chemistry*, *45*(10), 3840–3847.

Mua, J. P., & Jackson, D. S. (1997b). Relationships between functional attributes and molecular structures of amylose and amylopectin fractions from corn starch. *Journal of Agricultural and Food Chemistry*, *45*(10), 3848–3854.

Nakajima, M., Iwasaki, K. I., Nabetani, H., & Watanabe, A. (1990). Continuous hydrolysis of soluble starch by free β-amylase and pullulanase using an ultrafiltration membrane reactor. *Agricultural and Biological Chemistry*, *54*(11), 2793–2799.

Oechslein, C. R., Fricker, G., & Kissel, T. (1996). Nasal delivery of octreotide: Absorption enhancement by particulate carrier systems. *International Journal of Pharmaceutics*, *139*(1–2), 25–32.

Onofre, F., Wang, Y. J., & Mauromoustakos, A. (2009). Effects of structure and modification on sustained release properties of starches. *Carbohydrate Polymers*, *76*(4), 541–547.

Peppas, N. A., & Brannon-Peppas, L. (2001). Drug delivery biomaterials. In K. H. Jürgen Buschow, W. C. Robert, C. F. Merton, I. Bernard, J. K. Edward, M. Subhash, & V. Patrick (Eds.), *Encyclopedia of materials: science and technology* (2nd ed., pp. 2351–2355). Oxford: Elsevier.

Rahmouni, M., Lenaerts, V., Massuelle, D., Doelker, E., Johnson, M., & Leroux, J. C. (2003). Characterization of binary mixtures consisting of cross-linked high amylose starch and hydroxypropylmethylcellulose used in the preparation of controlled release tablets. *Pharmaceutical Development and Technology*, *8*(4), 335–348.

Reis, R. L., & Cunha, A. M. (2001). Starch polymers. In K. H. Jürgen Buschow, W. C. Robert, C. F. Merton, I. Bernard, J. K. Edward, M. Subhash, & V. Patrick (Eds.), *Encyclopedia of materials: science and technology* (2nd ed., pp. 8810–8815). Oxford: Elsevier.

Rindlav-Westling, Å., Stading, M., & Gatenholm, P. (2002). Crystallinity and morphology in films of starch, amylose and amylopectin blends. *Biomacromolecules*, *3*(1), 84–91.

Rindlav-Westling, A., Stading, M., Hermansson, A. M., & Gatenholm, P. (1998). Structure, mechanical and barrier properties of amylose and amylopectin films. *Carbohydrate Polymers*, *36*(2–3), 217–224.

Rindlav, A., Hulleman, S. H. D., & Gatenholm, P. (1997). Formation of starch films with varying crystallinity. *Carbohydrate Polymers*, *34*(1–2), 25–30.

Robin, F., Mérinat, S., Simon, A., & Lehmann, U. (2008). Influence of chain length on α-1,4-D-glucan recrystallization and slowly digestible starch formation. *Staerke[nl]Starch*, *60*(10), 551–558.

Smith, S. M., & Denyer, K. (2003). Primary products | starch. In T. Brian (Ed.), *Encyclopedia of applied plant sciences* (pp. 896–905). Oxford: Elsevier.

Subbotin, Y. N. Spline interpolation. *Encyclopedia of Mathematics*.

Tester, R. F., & Karkalas, J. (1996). Swelling and gelatinization of oat starches. *Cereal Chemistry*, *73*(2), 271–277.

Tuovinen, L., Peltonen, S., Liikola, M., Hotakainen, M., Lahtela-Kakkonen, M., Poso, A., et al. (2004). Drug release from starch-acetate microparticles and films with and without incorporated α-amylase. *Biomaterials*, *25*(18), 4355–4362.

Varshosaz, J. (2007). The promise of chitosan microspheres in drug delivery systems. *Expert Opinion on Drug Delivery*, *4*(3), 263–273.

Yokoyama, W., Renner-Nantz, J. J., & Shoemaker, C. F. (1998). Starch molecular mass and size by size-exclusion chromatography in DMSO-LiBr coupled with multiple angle laser light scattering. *Cereal Chemistry*, *75*(4), 530–535.

You, S., & Lim, S. T. (2000). Molecular characterization of corn starch using an aqueous HPSEC-MALLS-RI system under various dissolution and analytical conditions. *Cereal Chemistry*, *77*(3), 303–308.